

## Dynamic Structure in a Four-strategy Game: Theory and Experiment\*

Wang Zhijian<sup>1</sup>, Zhou Shujie<sup>1</sup>, Yao Qinmei<sup>1</sup>, Wang Yijia<sup>2</sup>, Pan Gang<sup>3</sup>

<sup>1</sup> *Zhejiang University, Experimental Social Science Laboratory,  
866, Yuhangtang Rd., Hangzhou 310058, China  
E-mail: wangzj@zju.edu.cn*

<sup>2</sup> *Ant Group,  
569, Xixi Road, Hangzhou, China*

<sup>3</sup> *Zhejiang University, College of Computer Science and Technology,  
866, Yuhangtang Rd., Hangzhou 310058, China*

**Abstract** Game dynamics theory, as any field of science, the consistency between theory and experiment is essential. In the past 10 years, important progress has been made in the merging of the theory and experiment in this field, in which dynamics cycle is the presentation. However, the achievement failed to eliminate the constraints of the Euclidean two-dimensional cycle. This paper uses a classic four-strategy game to study the dynamic structure (non-Euclidean superplane cycle). The consistency is in significant between the three ways: (1) analytical results from evolutionary dynamics equations, (2) agent-based simulation results from learning models and (3) laboratory results from human subjects game experiments. The consistency suggests that, the game dynamic structure could be quantitatively predictable, observable, and controllable in general.

**Keywords:** game theory; laboratory game experiment; eigenvector; eigenmode; dynamics system theory.

### 1. Introduction

#### 1.1. The background

In a discipline of science, the consistency between theory and experiment is essential. The two fundamental aspects of such consistency are accuracy and reality. As a scientific discipline, game theory, which attempts to explain strategy interactions among human subjects, is not an exception. We introduce the current conditions about the consistency of game theory as following.

Game statics theory, also called classical game theory, is the mainstream of game theory and centered around the concept – Nash equilibrium – established in 1950. Until 1987, human-subject game experiments (O’Neill, 1987) provided the first illustration that laboratory human strategy behavior can be accurately captured

---

\*This work was supported by the Science and Technology Innovation 2030 – “New Generation Artificial Intelligence” Major Project (No. 2018AAA0100900), China, and by the 985 Social Science foundation of Zhejiang University (2019).

An extended abstract has appeared in the 15th international conference on game theory and management (GTM2021), June 23–25, 2021, St. Petersburg, Russia. WZJ designed the research; ZSJ conducted the experiments and primer data analysis (for results, see her master’s thesis); and YQM and WYJ contributed to the associated experiment, critical data analysis, and manuscript writing. We thank Li Shijian, Fan Jijian, Jiamei Lian, Zheng Jie, Zhang Jianbo, Ke Rongzhu, Xu Bin, Chen Fadong, and Li Jingyuan for their helpful comments. WZJ especially thanks Shan Lixia for helping in manuscript preparation.

using this concept. Since then, this game has been extensively repeated in various experimental settings (Binmore et al., 2001; Okano, 2013). Based on this central concept, human subject behavior game theory and experiments have become a fruitful branch of academia (Camerer, 2003). As a result, game statics theory has been widely applied in real-life policy designs (mechanism design) to achieve certain social and economic objectives.

Game dynamics theory, which is based on evolutionary game theory, has been less developed over the last 50 years. In the past ten years, important progress has been made in the merging of theory and experiment (Cason et al., 2014; Wang et al., 2014; Xu et al., 2014; Cason et al., 2021). However, theoretical inferences and experimental measurements have failed to eliminate the constraints of two-dimensional Euclidean space (e.g., the theoretical expectation is two-dimensional (Cason et al., 2010; Xu et al., 2014; Cason et al., 2014; Wang et al., 2014) or measured in two-dimensions (Cason et al., 2021)). There is little evidence to bridge the gap between experiments and the theory of high-dimensional game dynamics.

Recently, it is found that the eigenmode (invariant manifold) plays a crucial role in human subject game experiments (Wang and Yao, 2020). In O'Neill game experiments, which state a space with eight dimensions (O'Neill, 1987; Binmore et al., 2001; Okano, 2013), the dynamic pattern in the experiments can be accurately interpreted using the eigenmode of the game dynamics equations (Wang and Yao, 2020). Guided by the replicator dynamics equations for the O'Neill game, the authors applied a complex eigenvector structure to interpret the dynamic structures in long-existing human game experiment data. The logic chain, which is rooted in the nonlinear dynamics theory (see Chapter 6 in Roussel, 2019), is as follows:

- For a given game, the game dynamics system can be expressed as a velocity vector field as (Sandholm, 2010; Friedman and Sinervo, 2016)

$$\dot{x} = f(x), \quad (1)$$

in which  $x \in R^N$  and  $N$  is the dimension of the strategy space;

- The Nash equilibrium is a singular point of the vector field (a point where  $\dot{x} = 0$ ). In linear approximation, near the singular point, the dynamics can be expressed as (Sandholm, 2010; Friedman and Sinervo, 2016)

$$\dot{x} = Jx,$$

in which  $J$  is the Jacobian (character matrix) at the singular point;

- Suppose that  $\xi_i$  is the eigenvector associated with the eigenvalue  $\lambda_i$  of the diagonalizable  $J$ ; and suppose that an initial condition can be expressed as  $x(0) = \sum_{i=1}^N a_i \xi_i$ . Then, the evolution trajectory can be expressed as

$$x(t) = \sum_{i=1}^N e^{\lambda_i t} a_i \xi_i. \quad (2)$$

Here, the eigenvector  $\xi_i$  describes an eigen mode, which is a normal mode in an oscillating system (which may have many components), wherein all parts of the components are oscillating with the same frequency  $\lambda_i$ ;

- If the system exists as an invariant manifold (eigen mode, a persist periodic orbit, and a persist loop), the manifold could be captured by a complex eigenvectors.

For a given complex eigenvector, disregarding the dimension of the game, there exists a measurement (constructed as an eigencycle set in theory and as angular momentum in experiment time series) to identify the invariant manifold. Here, the eigenvectors play the cruel role;

- Such that, a high dimension game dynamics structure is expected to be theoretically predictable and experimentally measurable.

By this logic chain, the fine dynamic structure in the existing data (O'Neill, 1987; Binmore et al., 2001; Okano, 2013) has been reported (Wang and Yao, 2020).

## 1.2. Motivation and the game selection

This research seeks to show that the dynamic behavior in human subject game experiments and game dynamics theory is consistent. Regarding the motivation and game selection of this study, we consider the following points:

1. In the long-existing data (O'Neill, 1987; Binmore et al., 2001; Okano, 2013) of the O'Neill game experiments, the high dimensional dynamics pattern meets the theory incredibly well; however, the evidence is unique (Wang and Yao, 2020)<sup>1</sup>. Is this consistency only a coincidence? We seek to solve this puzzle.
2. Regarding the game dynamics cyclic pattern, existing theoretical inferences and experimental measurements have not eliminated the constraints of the Euclidean two-dimensional space thus far (see Discussion 3.).
3. In game dynamics theory (Friedman and Sinervo, 2016; Sandholm, 2010), to obtain a superplane cycle, the game state space must have three independent variables. The candidate game is a one population four-strategy game, two population 2 + 3 strategy, or three population 2 + 2 + 2 game. For simplicity and no loss of generality, we choose a symmetric four-strategy game.

Therefore, we limited ourselves to a superplane cyclic game to investigate consistency between theory and experiments in the dynamic structure.

There exists a class of four-strategy games which being superplane cyclic in theory in textbooks (Hofbauer et al., 1998; Sandholm, 2010). Exemple figures can be seen in section '9.2.2 Continuation of Attractors for Parameterized Games' in Sandholm, 2010. The payoff matrix is presented in Table 1. We denote the payoff

**Table 1.** The four-strategy matrix

	$s_1$	$s_2$	$s_3$	$s_4$
$s_1$	0	0	0	$a$
$s_2$	1	0	0	0
$s_3$	0	1	0	0
$s_4$	0	0	1	0

matrix by  $A$ . The elements of matrix  $A(1, 4)$  are  $a$ . We define  $a$  as a positive number and control  $a$  to test whether the dynamic structure is predictable and controllable.

<sup>1</sup>After our experiment, an independent experiment reports (Yao, 2021) similar results as those found in the existing O'Neill game experiments (Wang and Yao, 2020). In this experiment, which is a one population five-strategy symmetric game with a unique pair of complex eigenvectors (eigen mode), the dynamics structure is also significantly consistent with the expectation of evolutionary dynamics theory (Yao, 2021)

In the state space (denoted by  $S$ ), one by one, we assign  $(x_1, x_2, x_3, x_4) \in S$  as the strategy probability of the strategy  $(s_1, s_2, s_3, s_4)$  used in the population. Subsequently, at any time ( $t$ ), the social state of the dynamic system must be a point in the four-dimensional space  $S(x_1, x_2, x_3, x_4)$ . In this four-dimensional space, we can verify that the unique mixed-strategy Nash equilibrium is:

$$x^* = (x_1^*, x_2^*, x_3^*, x_4^*) = \frac{1}{3a+1}(a, a, a, 1). \quad (3)$$

These are the basic aspects of a game.

In Section 2, we report the results in three ways: (1) We deduce the theoretical expectation from the eigensystem analysis; (2) we introduce the results of agent-based simulations; and (3) we introduce the results from the human subject game experiments. We then verify whether the theory and experiments are consistent. We conclude the study in Section 4.

## 2. Results

### 2.1. Results from dynamics models

**The eigen mode of the evolutionary dynamics** To investigate dynamic behavior in a laboratory experiment game, we begin by using replicator dynamics equations (Taylor and Jonker, 1978):

$$\dot{x}_i = x_i(U_i - \bar{U}), \quad (4)$$

where  $x_i$  is the  $i$ th strategy player probability in the population where the  $i$ th strategy player is included, and  $\dot{x}_i$  denotes the evolution velocity of probability.  $U_i$  is the payoff for the  $i$ th strategy player, and  $\bar{U}$  is the average payoff for the full population. This is a time-invariant, dynamic system. Suppose that the motion of strategy vector  $x$  is close to equilibrium and the linear approximation of dynamic system is validated. Then, we can obtain the eigensystem from the Jacobian (character matrix) (Sandholm, 2010; Friedman and Sinervo, 2016).

The Jacobian at the unique mixed-strategy Nash equilibrium of the dynamics in Eq. (4) can be calculated as follow:

$$J = \frac{a}{(3a+1)^2} \begin{pmatrix} -2a & -2a & -a-1 & 2a^2 \\ a+1 & -2a & -a-1 & -a(a+1) \\ -2a & a+1 & -a-1 & -a(a+1) \\ -2 & -2 & 2 & -a-1 \end{pmatrix}.$$

By the Jacobian, we can calculate the eigenvalues  $\lambda$  and their related eigenvector  $v$ 's components  $(\eta_1, \eta_2, \eta_3, \eta_4)$  explicitly. The eigenvalues  $\lambda$  are

$$\lambda = \frac{-a}{3a+1} \begin{pmatrix} i & 0 & 0 & 0 \\ 0 & -i & 0 & 0 \\ 0 & 0 & 1 & 0 \\ 0 & 0 & 0 & 1 \end{pmatrix}. \quad (5)$$

In dynamics system theory, this game is neutral because the maximum of the real part of the eigenvalues is 0. That is, in the replicator dynamics hypothesis, there exists a pair of purely imaginary eigenvalues; therefore, we will have *center invariant manifolds* associated with these eigenvalues.

Having the eigenvalue, we obtain the following related eigenvectors:

$$v = \begin{pmatrix} \frac{1}{4}(a - 1 + 3ai + i) & \frac{1}{4}(a - 1 - 3ai - i) & 0 & 1 \\ -\frac{1}{2}(a + 1) & -\frac{1}{2}(a + 1) & a & 0 \\ \frac{1}{4}(a - 1 - 3ai - i) & \frac{1}{4}(a - 1 + 3ai + i) & 0 & 1 \\ 1 & 1 & 1 & 0 \end{pmatrix} \tag{6}$$

Note that there exists a pair of conjugation complex eigenvalues, and naturally, their associated eigenvectors are pairs of conjugation complex eigenvectors. These complex eigenvectors determine the dynamic structure of the game. Using the explicit expression of the eigenvector shown in Eq. (6), the eigencycle can be obtained as follows.

**The eigencycle and rotation axis** Following the report (Wang and Yao, 2020), for an  $N$ -dimensional dynamics system, an eigencycle is constructed by two components  $(\eta_m, \eta_n)$  within a normalized eigenvector  $v_i = (\eta_1, \dots, \eta_m, \dots, \eta_n, \dots, \eta_N)^T$ . The eigencycle, denoted as  $\sigma^{(mn)}$ , is defined as follows:

$$\sigma^{(mn)} = \pi \cdot \|\eta_m\| \cdot \|\eta_n\| \cdot \sin(\arg(\eta_m) - \arg(\eta_n)), \tag{7}$$

where superscript  $(mn)$  is the index of the two-dimensional subspace, while  $m$  and  $n$  are the abscissa values and ordinate dimensions, respectively.  $\|\eta_m\|$  and  $\arg(\eta_m)$  indicate the amplitudes and a phase angle of  $\eta$ .  $\sigma^{(mn)}$  determines the direction of the eigencycle and the amplitude of the eigencycle. According to this formula, the eigenvalues of the eigenvectors in Eqs. (6) are

$$\sigma = \begin{pmatrix} \frac{1}{2}(a + 1) & -\frac{1}{2}(a + 1) & 0 & 0 \\ \beta & -\beta & 0 & 0 \\ -1 & 1 & 0 & 0 \\ \frac{1}{2}(a + 1) & -\frac{1}{2}(a + 1) & 0 & 0 \\ 0 & 0 & 0 & 0 \\ 1 & -1 & 0 & 0 \end{pmatrix}, \tag{8}$$

where  $\beta = \frac{5a^2+2a+1}{6a+2} \left[ \sin\left(\arg\left(\frac{a-1}{4} - \frac{3a+1}{4}i\right) - \arg\left(\frac{a-1}{4} + \frac{3a+1}{4}i\right)\right) \right]$ . Notably, (1) for the eigencycle values, referring to a real eigenvalue, is zero because  $\arg(\eta_m)$  is equal to  $\arg(\eta_n)$ . In other words, the related eigenvector components showed no phase differences. (2) The pair of the eigencycle set, which is associated with a pair of complex conjugation eigenvectors, has opposite values. Interestingly, if we disregard the value  $a$ , the following relationship holds:

$$\sigma^{24} = 0, \tag{9}$$

$$\sigma^{14} = -\sigma^{34}, \tag{10}$$

$$\sigma^{12} = \sigma^{23}. \tag{11}$$

In section 2.2. on the results from human subject experiments, these relationships (independent of the  $a$  relationship or the  $a$ -invariant relationship) are tested statistically (see Figure 3).

Referring to the report (Wang and Yao, 2020), we interpret the eigencycle and parameter selection for this study as follows:

- **Number of eigencycle:** The number of the independent eigencycle in this study is 6. Based on its definition, for an  $N$ -dimensional system, there are  $N(N-1)/2$  independent eigencycles corresponding to a given  $N$ -component normalized eigenvector, as there exist a total of  $N^2$  pairwise combinations of each component in an  $N$ -dimensional eigenvector. Considering that the  $N$  self-combinations of  $(\eta_m, \eta_m)$  are trivial ( $\sigma^{(mm)} = 0$ ), and  $(\eta_m, \eta_m)$  and  $(\eta_m, \eta_m)$  are simply the reversed ( $\sigma^{(mn)} = -\sigma^{(nm)}$ ), only  $N(N-1)/2$  independent combinations remain. Further,  $N = 4$ ; hence, the number of the eigencycle is 6.
- **Eigencycle set:** In this study case, there is only one independent eigencycle set (see the first column in the eigenvector matrix  $\sigma$ ), as there is only one pair of conjunction complex eigenvalues (see the first and second diagonal elements of the eigenvalue matrix in  $\lambda$ ). The associated complex eigenvector is a pair of conjunction complex vectors (see first and second column of the eigenvector matrix in  $v$ ). The eigencycle set is defined to represent the set of  $N(N-1)/2$  eigencycle elements. The superscript  $(mn)$  is the index of the two-dimensional subspace where the elements (eigencycles) of the set are located.  $(mn)$  is defined as  $\{\{m, n\} \in \{1, 2, \dots, n\} \cap (m < n)\}$ . The assignment order is  $m$  from 1 to  $N$  first, and then  $n$  from 2 to  $N$ .
- **The parameter selection:** As per the definition of the eigencycle, changing  $a$  in the game matrix  $A$  will change the values of the six eigencycles. The results are shown in Figure 1. We choose the parameters we do for the following reasons: (1) To properly verify the real human subject experiments, the parameter needs to be simple and understandable. (2) Various parameters require various treatments, and the theoretical expectations will require significant differences between the various treatments. As a result, we choose  $a = [1/4, 4]$  as the two treatments as the focus of our investigation.
- **Geometric presentation:** Figure 2 illustrates the ideal cyclic motion of the replicator dynamics (see Eq. (4)) for the game (see Table 1) with  $a = [1/4, 4]$  near the Nash equilibrium. The geometric presentation of an eigencycle is similar to (1:1)-Lissajous diagrams. In the (1:1)-Lissajous diagram, the amplitude of two components can be arbitrary, but the amplitude of two components of an eigencycle in a dynamic system at equilibrium is fixed and not arbitrary owing to the natural constrain of the eigenvector components. At the same time, the eigencycle only depends on the internal components  $\eta_m$  and  $\eta_n$ , which belong to the unique complex eigenvector. Following the reference (Roussel, 2019), the cycle can be regarded as the projection of the eigen-trajectory in the two-dimensional Euclidean spaces.

The rotation axis can be used as a measurement for a four-strategy game because the constraint condition of the state space of a one population game is  $\sum_{i=1}^4 x_i = 1$ . Therefore, the trajectory of dynamic processes can be fully presented by three-dimensional variables  $(x_1, x_2, x_3)$ . In this study, the rotation axis is a vector, defined as the vector of the angular momentum. In other words, the rotation axis vector components are defined as exactly equal to the angular momentum vector components. An explanation of the definition of the measurement, as well as of the calculation approach for the theoretical results, is shown in Appendix 4.5.

Using the procedure illustrated from Eq. (4) to Eq. (8), we can calculate the Eigencycle values and the axis direction of a given dynamic equation system. In addition to the replicator dynamics, which are labeled as  $[T_1]$ , we select the MS-

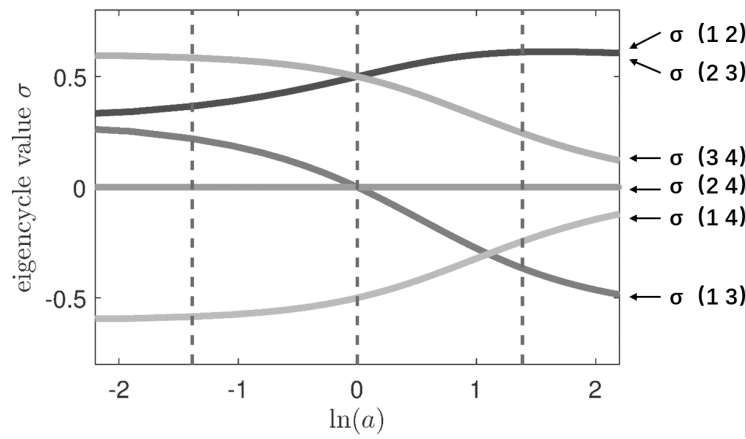


**Fig. 1.** Theoretical prediction of the eigencycle value referring to  $a$ . For symmetric visibility, the horizon axis is scaled with the natural log function. These curves represent the eigencycles values of the replicator dynamics shown in Eq. (4) for the four-strategy (symmetric one population) game with the payoff matrix shown in Table 1. The left-most and right-most dashed lines indicate the  $a = [1/4]$  and  $a = [4]$  conditions (treatment) that we shall investigate in theory and experiments, respectively

replicator dynamics (labeled as  $[T_2]$ , and also called adaptive replicator dynamics) and logit dynamics (also called noise best response dynamics). In logit dynamics, to illustrate the dynamics pattern referring to the noise level, we select three noise parameters ( $[0.001, 0.05, 300]$ ) that are labeled as  $[T_3, T_4, T_5]$ .

In summary, the theoretical expectations can be calculated for the five dynamic models (and parameters). The theoretical expectations for the Eigencycle set are shown in Table 2 in the rows labeled as  $[T_1, T_2, T_3, T_4, T_5]$ . The rotation axis vector components of the theoretical expectations are listed in Table 3 in the rows labeled  $[T_1, T_2, T_3, T_4, T_5]$ .

**2.2. Results from human subject experiment**

We conducted a laboratory game experiment with human subjects to investigate the game dynamics structure. Two treatments were used in the experiment. The parameters of  $a$  in the games were  $1/4$  and  $4$ , respectively. Eight sessions were conducted for each treatment. Each session includes a game repeated over 1,000 periods, with each lasting about 2.5 to 3 hours. The average payment for each subject was RMB 150. Each session included six subjects. The game matching protocol was random; in every period, the counterpart of a subject was randomly selected from one of the other five subjects, which is the same as (Wang et al., 2014). The details of the experimental protocol are provided in Appendix 4.2.

There were 8,000 rounds of time series for each of the two treatments. We use the time series to measure the eigencycles and rotation axis direction for each of the two treatments  $a = [1/4, 4]$ .

- For the eigencycle set, the results of the human subject game experiments are shown in Table 2 in the row labeled  $[E]$ .
- For the rotation axis vector components, the results are shown in Table 3 in the row labeled  $[E]$ .

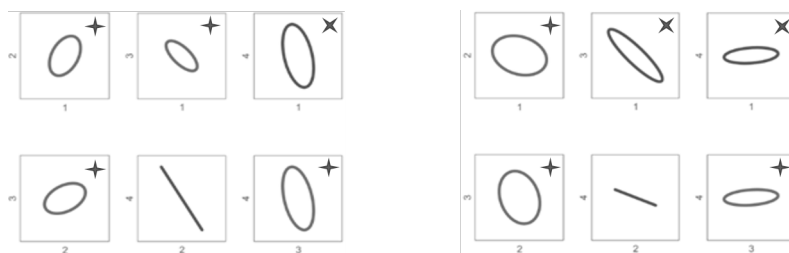


**Fig. 2.** The geometric presentation of the eigencycle values  $\sigma_{mn}$  of the six two-dimensional subspace. Results come from the replicator dynamics (see Eq. (4)) for the game (see Table 1), in which left panel  $a = [1/4]$  and right panel  $a = [4]$ . The symbol  $\times$  (blue in electronic version) indicates the cycle is clockwise with negative value, and the symbol  $+$  (red in electronic version) indicates the cycle is counter-clockwise with positive value. The relative value of the areas of the six cycles is the relative value of the six eigencycles. The angular momentum  $L_{mn}$  measures the subspaces in the time series of the experiment and should be proportional to the  $\sigma_{mn}$  value (the proof has been shown in the report (Wang and Yao, 2020))

- As a response to the strict relationship of the independence of  $a$  shown in Eq. (10) and Eq. (11), we show the relationship from the data in Figure 3. Obviously, the relationships hold, with significance.
- As a response to the strict relationship of the independence of  $a$  shown in Eq. (9), the statistical results show that the prediction cannot be rejected by data (*ttest*,  $p=0.6029$ , sample size  $N=8$  in  $a = 1/4$  treatment; *ttest*,  $p=0.2239$ , sample size  $N=8$  in  $a = 4$  treatment).

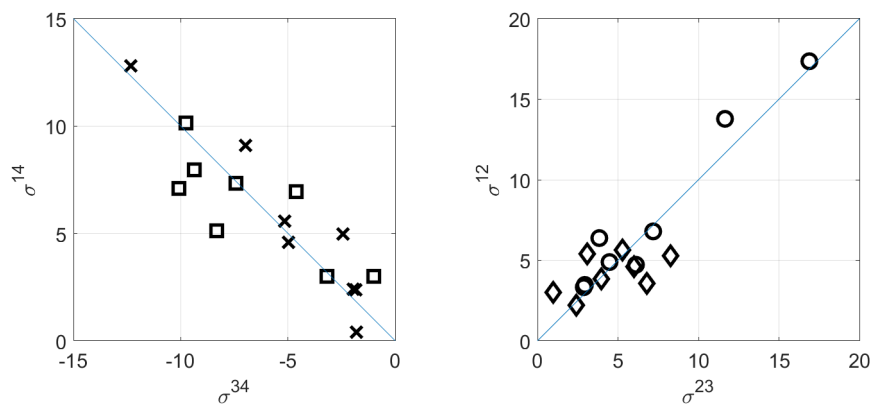


**Fig. 3.** The relationship of the independence of  $a$  between the observations. Scatter experiment eigencycle values shown in the left panel support the relationship predicted in Eq. (10), wherein the square indicates the  $a = 1/4$  treatment and the cross indicates the  $a = 4$  treatment. The scatter experiment eigencycle values shown in the right panel support the relationship predicted in Eq. (11), wherein the circle indicates the  $a = 1/4$  treatment and the diamond indicates the  $a = 4$  treatment. Notice that, as each treatment includes eight repeated sessions, each scattering has eight samples

**2.3. Results from agent-based simulation**

To investigate the dynamic structure, we hope to obtain results from agent-based reinforcement learning models. We use the agent-based evolutionary dynamics (ABED) simulator (Izquierdo et al., 2019), which is widely used to study evolutionary game dynamics. The platform integrates various learning rules and matching rules, covering the mainstream dynamics model of evolutionary dynamics. This is an ideal platform to simulate the dynamics process for various models.

**Table 2.** The eigencycles of theory ( $T$ ), human experiment ( $E$ ) and simulation ( $S$ )

	$\sigma_{12}$	$\sigma_{13}$	$\sigma_{14}$	$\sigma_{23}$	$\sigma_{24}$	$\sigma_{34}$
$E$ : Human Exp.						
$a=1/4$	0.0046	0.0021	-0.0067	0.0042	0.0004	0.0063
$a=4$	0.0070	-0.0024	-0.0047	0.0076	-0.0006	0.0053
$S_1$ : Replicator						
$a=1/4$	0.0004	0.0002	-0.0006	0.0004	0	0.0006
$a=4$	0.0002	-0.0001	-0.0001	0.0002	0	0.0001
$S_2$ : MSReplicator						
$a=1/4$	0.0565	0.0073	-0.0639	0.0560	0.0005	0.0633
$a=4$	0.0728	-0.0212	-0.0516	0.0723	0.0005	0.0511
$S_3$ : Logit[0.001]						
$a=1/4$	0.0023	0.0009	-0.0032	0.0026	-0.0003	0.0035
$a=4$	0.0091	-0.0047	-0.0044	0.0089	0.0002	0.0042
$S_4$ : Logit[0.05]						
$a=1/4$	0.0021	0.0008	-0.0030	0.0025	-0.0003	0.0033
$a=4$	0.0081	-0.0042	-0.0039	0.0079	0.0001	0.0037
$S_5$ : Logit[300]						
$a=1/4$	0.1735	-0.8947	0.7212	-0.7455	0.919	-1.6402
$a=4$	1.5904	-0.4227	-1.1677	0.1526	1.4378	-0.2701
$T_1$ Replicator						
$a=1/4$	0.4659	0.2795	-0.7454	0.4659	0	0.7454
$a=4$	0.8653	-0.5192	-0.3461	0.8653	0	0.3461
$T_2$ MSReplicator						
$a=1/4$	0.4659	0.2795	-0.7454	0.4659	0	0.7454
$a=4$	0.8653	-0.5192	-0.3461	0.8653	0	0.3461
$T_3$ Logit[0.001]						
$a=1/4$	0.4648	0.2809	-0.7457	0.4658	-0.0010	0.7467
$a=4$	0.8662	-0.5202	-0.3461	0.8658	0.0004	0.3457
$T_4$ Logit[0.05]						
$a=1/4$	0.4133	0.3160	-0.7292	0.4796	-0.0663	0.7957
$a=4$	0.9072	-0.5527	-0.3547	0.8790	0.0284	0.3263
$T_5$ Logit[300]						
$a=1/4$	0.5282	0.1730	-0.7012	0.7576	-0.2294	0.9306
$a=4$	0.9455	-0.3220	-0.6234	0.7331	0.2123	0.4111

As mentioned above, there are five models (the replicator dynamics, which are labeled as  $S_1$ ; MS-replicator dynamics, which are labeled as  $S_2$ ; and the three noise parameter [0.001, 0.05, 300] logit dynamics models, labeled as  $S_3, S_4,$  and  $S_5,$  respectively) for the two ( $a \in [1/4, 4]$ ) treatments. Therefore, we used ten independent simulation protocols. For each protocol, there were  $10^5$  rounds of time-series. We

**Table 3.** The rotation axis vector components of theory ( $T$ ), human experiment ( $E$ ) and simulation ( $S$ )

Treatment Axis	$a=1/4$			$a=4$		
	1	3	2	1	3	2
Analytical						
$T_1$ : Replicator	-0.0212	-0.0212	0.0127	-0.0847	-0.0847	-0.0508
$T_2$ : MSReplicator	-0.1483	-0.1483	0.089	-0.2754	-0.2754	-0.1653
$T_3$ : Logit[0.001]	-0.0001	-0.0001	0.0001	-0.0004	-0.0004	-0.0002
$T_4$ : Logit[0.05]	-0.2038	-0.1756	0.1342	-0.7953	-0.8209	-0.5
$T_5$ : Logit[300]	-0.0001	-0.0001	0	-0.0001	-0.0002	-0.0001
Simulation						
$S_1$ : Replicator	-0.0004	-0.0004	0.0002	-0.0002	-0.0002	-0.0001
$S_2$ : MSReplicator	-0.056	-0.0565	0.0073	-0.0723	-0.0728	-0.0212
$S_3$ : Logit[0.001]	-0.0026	-0.0023	0.0009	-0.0089	-0.0091	-0.0047
$S_4$ : Logit[0.05]	-246.2	-214.5	81.87	-790.9	-805.9	-417.8
$S_5$ : Logit[300]	0.7455	-0.1735	-0.8947	-0.1526	-1.5904	-0.4227
Human Exp.						
$E$ : mean	-0.0042	-0.0046	0.0021	-0.0076	-0.007	-0.0024

used the time series to measure the eigenvalues and direction of the rotation axis. The details of the simulation protocols are provided in Appendix 4.3..

Label the agent-based simulation with the protocol following the replicator dynamics setting as ( $S_1$ ), the MS replicator dynamics setting as ( $S_2$ ), and the logit dynamics setting with noise parameter [0.001, 0.05, 300] as ( $S_3, S_4, S_5$ ); the results are reported from the time series.

- For the eigencycle set, the results of the simulation are shown in Table 2 in the rows labeled [ $S_1, S_2, S_3, S_4, S_5$ ].
- For the rotation axis vector components, the results are shown in Table 3 in the rows labeled [ $S_1, S_2, S_3, S_4, S_5$ ].

#### 2.4. Consistency of theory and experiment

The consistency of the dynamic structure between the experiment, theory, and simulation were the central questions in this study. To answer this question, we identified the dynamic structure by the eigencycle (the result is shown in 2) and the direction of the rotation axis (the result is shown in 3). We now calculate the correlation coefficients of the observations (the eigencycle set and direction of the rotation axis) of the experiment, theory, and simulation to report the statistical results on the consistency.

- Regarding the eigencycle measurement, the consistency between the theory and experiment is significant. The supporting data with explanation are as follows.
  - The data of the eigencycle set of the experiment, the five-theory model, and five-agent based models simulation are shown in Table 2. We calculate the correlation coefficients for the two treatments  $a = [1/4, 4]$ , respectively. For  $a = [1/4]$ , the results are reported in Table 4; and for  $a = [4]$ , the results are reported in Table 5. For visibility, we strike out coefficients smaller than 0.900.

- It is obvious that, except for extremely high noise conditions  $S_5$  and  $T_5$  (noise parameter is 300) of the logit dynamics model, the experiment and theory and simulation are significantly consistent ( $\rho > 0.900$ ,  $N = 6$ ). Importantly, the experiment results can be soundly interpreted by the models in the  $a = [1/4]$  treatment (see the first column in Table 4) and in the  $a = [4]$  treatment (see the first column in Table 5). The consistency of theory and experiment is supported with strong significance ( $\rho > 0.950$ ,  $N = 6$ ).
- Figure 4 illustrates the relationship of the normalized theoretical and the normalized experimental eigencycles for the two ( $a = [1/4, 4]$ ) treatments. By ordinary linear regression, the match between the theory and experiment is significant ( $p = 0.000$  for  $a = [1/4]$  treatment,  $p = 0.003$  for  $a = [4]$  treatment, the sample size of each treatment  $N = 6$ ).

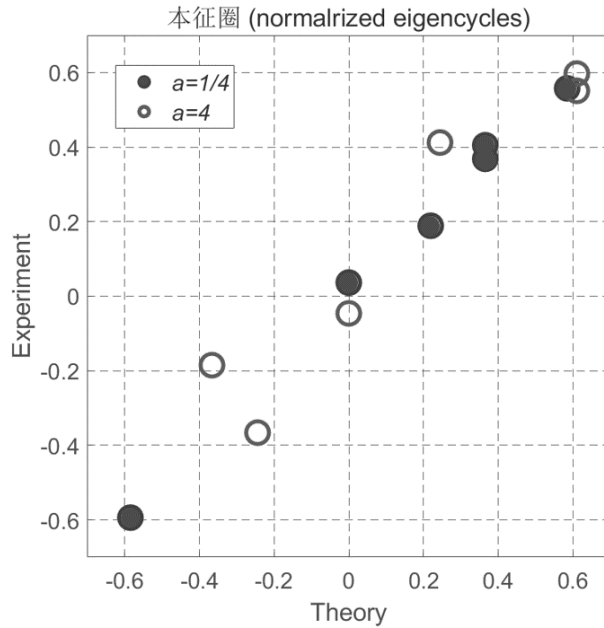


**Fig. 4.** Relationship of the normalized theoretical and the normalized experimental eigencycles for the two ( $a = [1/4, 4]$ ) treatments. The normalized theoretical eigencycles results come from the replicator dynamics model  $T_1$ . In the normalization, the six components are divided by the root of the sum of their square. For  $T_2, T_3, T_4$  and  $S_1, S_2, S_3, S_4$ , the relationship is similar

- Regarding the measurement of the rotation direction axis vector components, the march between the theory and experiment is significant. The supporting data are as follows:
  - The rotation direction axis vector components of the experiment, the five-theory model, and five-agent based models simulation are shown in Table 3. We calculate the correlation coefficients for the two treatments  $a = [1/4, 4]$ , respectively. For  $a = [1/4]$ , the results are reported in Table 8; and for  $a = [4]$ , the results are reported in Table 9. For visibility, we strike out coefficients smaller than 0.900.

- It is obvious that, except for extremely high noise conditions [ $S_5, T_5$ ] (noise parameter is 300) of the logit dynamics model, all the theory and simulation are consistent. Importantly, the experiment results can be well interpreted by the models in the  $a = [1/4]$  treatment (see the first column in Table 8) and in the  $a = [4]$  treatment (see the first column in Table 9) in section 4.6. of the Appendix.

In summary, these two measurements provide the same conclusion that, in general, the game dynamics structure can be captured significantly by the game dynamics model in human subject game experiments.

**Table 4.** The correlation coefficients of the eigencycles of theory ( $T$ ), human experiment ( $E$ ), and simulation ( $S$ ) for  $a = [1/4]$

	$E$	$S_1$	$S_2$	$S_3$	$S_4$	$S_5$	$T_1$	$T_2$	$T_3$	$T_4$	$T_5$
$E$	1										
$S_1$	0.998	1									
$S_2$	0.980	0.979	1								
$S_3$	0.990	0.995	0.986	1							
$S_4$	0.988	0.993	0.986	1.000	1						
$S_5$	-0.697	-0.733	-0.640	-0.751	-0.755	1					
$T_1$	0.997	0.999	0.969	0.991	0.990	-0.748	1				
$T_2$	0.997	0.999	0.969	0.991	0.990	-0.748	1.000	1			
$T_3$	0.997	0.999	0.969	0.991	0.989	-0.749	1.000	1.000	1		
$T_4$	0.987	0.993	0.955	0.989	0.988	-0.804	0.996	0.996	0.996	1	
$T_5$	0.953	0.966	0.967	0.986	0.988	-0.804	0.960	0.960	0.960	0.968	1

**Table 5.** The correlation coefficients of eigencycles of theory ( $T$ ), human experiment ( $E$ ), and simulation ( $S$ ) for  $a = [4]$

	$E$	$S_1$	$S_2$	$S_3$	$S_4$	$S_5$	$T_1$	$T_2$	$T_3$	$T_4$	$T_5$
$E$	1										
$S_1$	0.980	1									
$S_2$	0.997	0.976	1								
$S_3$	0.973	0.999	0.971	1							
$S_4$	0.973	0.999	0.970	1.000	1						
$S_5$	0.482	0.552	0.546	0.568	0.566	1					
$T_1$	0.953	0.994	0.947	0.996	0.996	0.547	1				
$T_2$	0.953	0.994	0.947	0.996	0.996	0.547	1.000	1			
$T_3$	0.953	0.994	0.947	0.996	0.996	0.548	1.000	1.000	1		
$T_4$	0.944	0.991	0.940	0.994	0.995	0.570	0.999	0.999	0.999	1	
$T_5$	0.954	0.968	0.972	0.969	0.968	0.720	0.949	0.949	0.949	0.950	1

### 3. Discussion

This report illustrates that the dynamic behaviors in the human subject game experiment and the game dynamics theory are consistent. The main contributions of this study are as follows: (1) The non-Euclidean superplane cycle is confirmed for the first time. (2) The report (Wang and Yao, 2020) of the findings from the O'Neill

game (O'Neill, 1987; Binmore et al., 2001; Okano, 2013) is not a coincidence, but also validates in the four-strategy game experiment case. (3) The characteristics of the game dynamic cycle can be predictable, observable, and controllable in a human game experiment.

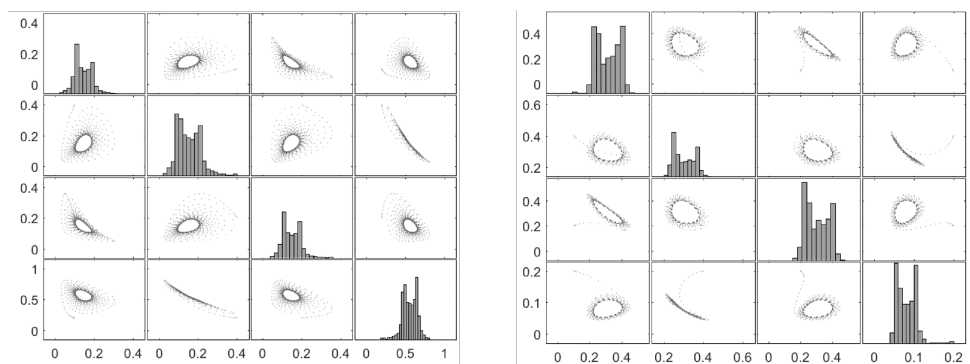


**Fig. 5.** Matrix scatter plot of a sample evolutionary trajectory projected to the two-dimensional subspace of the state space. The trajectory (time series) is generated by the replicator dynamics equations with a random initial condition. It is obvious that, in the so-called cycle, the closed period orbit is not in a Euclidean plane. In both treatments, in the  $(x_2, x_4)$ -subspace, the projections of the orbit are not straight-lined segments, but curved segments. The left and right panels are of treatment  $a = [1/4, 4]$ , respectively

**On related works.** To our knowledge, the match of the theory and experiment has not eliminated the constraints of the Euclidean two-dimensional space thus far. The past ten years have seen quantitative matching between theory and experiment on game dynamics, but of all published works, the theoretical expectations are actuarial of the Euclidean two-dimension (Cason et al., 2010; Xu et al., 2014; Cason et al., 2014; Wang et al., 2014). Even in four-strategy games experiments (Cason et al., 2010; Van Huyck et al., 1999), the concerned cycles are in the Euclidean plane. In the price dynamics cycle investigation, the price as a strategy is continuous; however, the theoretical expectation and experimental measurement are projected onto the Euclidean two-dimensional plane for verification (Cason et al., 2021)).

The game selected in this study is a superplane (or twisted plane) and not an ordinary two-dimensional Euclidean plane. This can be seen in Figure 5, wherein the projection of the persistent cycle is not a straight-lined segment but a curved one. Both  $a = [1/4, 4]$  treatments have the same performance. Therefore, we call this cycle a superplane cycle.

**On further work.** In the human subject experiment, there exists a structural difference between the experimental strategy distribution, which deviates from the theoretical expectation show in Eq. (3). This is a puzzle. The details of the distribution deviation observed in the experiments can be the thesis (Zhou, 2021). Second, the axis or direction of rotation under different parameters can only be qualitatively differentiated using angular momentum. Identifying the curve rate of the segment (which is the theoretical expectation shown in Figure (5)) in this experiment was unclear. Together, these issues are related to the consequences of the evolution trajectory on the distribution of a game. Naturally, as a metaphor, further investigation

into real strategy interaction systems would make game dynamics more accurate, understandable, and applicable.

**On dynamics structure control.** We realize the control of the dynamics structure by controlling the parameter  $a$ . This is different from the existing literature (Cason et al., 2010; Xu et al., 2014; Cason et al., 2014; Wang et al., 2014), wherein the object of control is the eigenvalue for various stabilities. In this study, the object of control was the eigenvector. We control the cycle structure by controlling the payoff matrix element  $a$ . To our knowledge, this report provides a new realization of the game mechanism design for dynamic structures. Control-by-design is a critical issue not only in engineering but also in game theory, namely, mechanism design.

Considering that the dynamic structure (eigenvector, invariant manifold, and eigenmode) is associated with the business cycle in macroeconomics and microeconomics (Schoonbeek, 1987; Iyetomi et al., 2020), the control of a dynamic structure is not a trivial issue. During this study, we noticed that using the five-strategy game (Wang and Yao, 2020) experiments as the benchmark and the pole assignment approach in modern game theory (which is a state-dependent closed-loop feedback design), the control of the dynamic structure was proved to be significant (Wang, 2022). Noticeably, when we change the control variable  $a$  of the game, the dynamic structure changes along with the equilibrium of the game as well. Alternatively, in a closed-loop feedback control (Wang, 2022), when the dynamic structure changes, the equilibrium does not change. At the same time, no additional financing is required during the control process.

#### 4. Appendix

The methods used in this study include the following: (1) five-game dynamic system equations, (2) agent-based simulation of evolutionary game dynamics, and (3) laboratory human subject game experiment. Simultaneously, in the measurement, we used (1) the direction of the axis of rotation and (2) the eigencycle. In this section, we describe these methods in detail.

##### 4.1. The five-game dynamics models

There are five models (dynamic system equations) with the parameters applied to illustrate the match between theory and experiments. They are the (1) replicator dynamics, labeled as  $[T_1]$  in the main text; (2) MS-replicator dynamics, which are labeled as  $[T_2]$  in the main text; and (3) logit dynamics (also called noise best response dynamics). In logit models, we select three noise parameters ( $[0.001, 0.05, 300]$ ), which are labeled  $[T_3, T_4, T_5]$  in the main text. The dynamic equations are presented as follows:

- Replicator Dynamics

$$\dot{x}_i = x_i(U_i - \bar{U}), \quad (12)$$

where  $\dot{x}_i$  is the velocity of the proportion growth of the population using  $i$ th strategy,  $U_i$  is the payoff of an agent in the population using  $i$ th strategy, and  $\bar{U}$  indicates the mean payoff of the population. In the main text, this model is denoted as  $[T_1]$ . For one population symmetric game with payoff matrix  $A$ , we have

$$U_i = \sum_{j=1}^N A_{ij}x_j \quad (13)$$

and

$$\bar{U} = \sum_{i=1}^N x_i U_i. \quad (14)$$

- MS replicator dynamics are the adjusted replicator dynamics.

$$\dot{x}_i = \frac{x_i(U_i - \bar{U})}{\bar{U}}, \quad (15)$$

where  $\dot{x}_i$  is the velocity of the population using  $i$ ,  $U_i$  is the payoff of an agent in the population  $i$ , and  $\bar{U}$  indicates the mean payoff in the population. For the algorithm for  $U_i$  and  $\bar{U}$ , see Eq. (13) and Eq. (14). In the main text, this model is denoted as  $[T_2]$ .

- Logit dynamics is the noise best response model.

$$\dot{x}_i = \frac{\exp(\lambda U_i)}{\sum_{j=1}^N \exp(\lambda U_j)} - x_i, \quad (16)$$

where  $\lambda$  is the noise parameter,  $\dot{x}_i$  is the velocity of the population using  $i$ , and  $U_i$  is the payoff of an agent in the population  $i$ . For the algorithm for  $U_i$ , see Eq. (13). In the main text,  $[T_3, T_4, T_5]$  relates to the  $\lambda = [0.001, 0.05, 300]$  condition, respectively.

#### 4.2. Human subject game experiment protocol

The experiment was approved by the Experimental Social Science Laboratory of Zhejiang University. The data for the controlled treatment ( $a = [1/4, 4]$ -Treatment) are from the experiment conducted from November to December 2020. The authors confirm that this experiment was performed in accordance with the approved social experiment guidelines and regulations, which follow the regulation of the **experimental economics** protocol (Camerer, 2003).

In total, 96 undergraduate and graduate students of Zhejiang University volunteered to serve as the human subjects of this experiment. Students were recruited openly through a web registration system.

The 96 human subjects (also called players) were distributed into 16 populations of equal sizes, with  $N = 6$ . The six players of each population carried one experimental session (see the session organization table). During the game process, the players sat separately in a classroom laboratory, each facing a computer screen. They were not allowed to communicate with each other during the experimental session. Written instructions were handed out to each player and the rules of the experiment were explained orally by an experimental instructor. The rules of the experimental session were as follows:

1. Each player plays the four-strategy game repeatedly with the same other five players.
2. Each player earns virtual points during the experimental session according to the payoff matrix shown in the written instruction.
3. In each game round, each player competes with one player and the other five players as the opponent.
4. Each player has to make a choice among the four candidate actions<sup>4</sup>, “x1<sup>x</sup>,” “x2<sup>x</sup>,” “x3<sup>x</sup>,” and “x4<sup>x</sup>.” If this time runs out, the player has to make a choice immediately. After a choice has been made, it cannot be changed.



**Fig. 6.** The screenshot of the user interface in human subject game experiment. The left panel is an example. The subject ID is T001, whose history information is at the 999<sup>th</sup> round in the top. The current round's strategy options are at the bottom. The right panel is the English translation of the left

**Table 6.** The experiment session organization

$a=1/4$				$a=4$			
SessionID	Date	Subjects	Period	SessionID	Date	Subjects	Period
01121A251	20201121	6	1000	01122A441	20201122	6	1000
01121A252	20201121	6	1000	01122A442	20201122	6	1000
01122A253	20201122	6	1000	01128A443	20201128	6	1000
01122A254	20201122	6	1000	01128A444	20201128	6	1000
01128A255	20201128	6	1000	01129A445	20201129	6	1000
01129A256	20201129	6	1000	01129A446	20201129	6	1000
01219A258	20201219	6	1000	01219A448	20201219	6	1000
01227A250	20201227	6	1000	01228A449	20201228	6	1000

During the experimental session, each player's computer screen displayed an information window and a decision window. The window on the left side of the computer screen is the information window. The upper panel of this information window shows the current game round, the time limit (40 s in controlled ( $a = [1/4, 4]$ -Treatment)) for making a choice, and the time left to make a choice. The upper panel turns green at the start of each game round. After all players have made their decisions, the lower panel of the information window shows the player's own choice, opponent strategy, and payoff in this game round on the screen. The player's accumulated payoff is also shown. The players were asked to record their choices for each round on the record sheet in some rounds for checking. Each session lasts 2.5–3 hours, with more than 1,000 period records per session. For each  $a = [1/4, 4]$  treatment, eight sessions were repeated. Thus, we had 8,000 records in the time series for each treatment.

The window on the right side of the computer screen is the decision window. It is activated only after all players in the group have made their choices. The upper panel of this decision window lists the current game round, while the lower panel lists the four candidate actions (“x1<sup>x<sub>t</sub></sup>,” “x2<sup>x<sub>t</sub></sup>,” “x3<sup>x<sub>t</sub></sup>,” and “x4”) horizontally from left to right. The player can choose by clicking on the corresponding action names.

The reward for each player is determined by the rank, which is determined by the total number of earning points in the experimental sessions. From the highest

to the lowest, each player is paid RMB 275, RMB 225, RMB 175, RMB 125, RMB 75, and RMB 25 in the controlled treatments.

#### 4.3. Agent-based evolutionary dynamics simulation protocol

Reinforcement learning theory is a branch of gaming theory. Agent-based evolutionary dynamics simulation is an approach for understanding the consequences of reinforcement learning theory. The computer simulation method to evaluate the consistency of the theory and experiment is introduced as follows.

1. **Select simulation platform.** We use abed simulator (Izquierdo et al., 2019), which is widely used in the field to study evolutionary game dynamics. The platform has integrated various learning rules and matching rules and has covered the mainstream dynamics model of evolutionary dynamics, which is an ideal platform to simulate the dynamic process. The platform is a long-running, repeated game setting in finite populations.
2. **Setting parameters.** The parameter settings for the five simulations are listed in Table 7. The authors carefully classified (approximate) equivalence between the dynamic evolutionary equations and parameter settings for simulation. For example, for the replicator dynamics model, the simulation is under imitative protocols in which candidates are agents; meanwhile, the decision method is a pairwise comparison of the strategy payoff. Complete matching was performed. These settings follow the user guide of the platform, which the system performs as replicator dynamics, as shown in Eq. (4), for a large population (1,000 agents) and a low reversion probability (1%) limit.
3. **Conducting the simulation.** In our case study, for each of the five models and each of the treatments investigated, we ran a 1M period simulation. The time cost for each run of the simulation of a given parameter set was approximately 30 min on a desktop personal computer with a CPU of 8 GHz and a memory of 16 GB.
4. **Analysis of the time series.** The main outcome of the simulator is the time series. The time series, including the strategy density and their payoffs, can be the output from the platform. These can be used to evaluate the performance of the controller-by-design, for example, fluctuation as well as the efficiency, profits, or social welfare evolution over time.

#### 4.4. Angular momentum as the measurement

According to the theoretical eigencycle set decomposition approach, we can perform cyclic angular momentum measurements in each of the two-dimensional subspace, indicated by the eigencycle  $\Omega^{(mn)}$ . Angular momentum  $L_E^{(mn)}$  (Wang et al., 2017) can be expressed by the following formula:

$$L_E^{mn} = \frac{1}{N-1} \sum_{t=1}^{N-1} (x(t) - O) \times (x(t+1) - x(t)). \quad (17)$$

- $L_E^{(mn)}$  represents the average value of the accumulated angular momentum over time; the subscript  $mn$  indexes the two-dimensional  $(x_m, x_n)$  subspace;
- $N$  is the length of the experimental time series, that is, the total number of repetitions of the repeated game experiments;
- $O$  is the projection of the Nash equilibrium at the subspace  $\Omega^{(m,n)}$ ;

**Table 7.** The parameter setting for the five models' simulations

Parameter	Replicator [ $S_1$ ]	MS-Replicator [ $S_2$ ]	Logit [ $S_3, S_4, S_5$ ]
payoff-matrix	[[ 0 0 0 4 ] [ 1 0 0 0 ] [ 0 1 0 0 ] [ 0 0 1 0 ]]	as left	as left
n-of-agents	1000	1000	1000
random-initial-condition?	FALSE	FALSE	FALSE
initial-condition	[250 250 250 250]	[250 250 250 250]	[250 250 250 250]
candidate-selection	imitative	imitative	imitative
n-of-candidates	2	2	2
decision-method	pairwise-difference	positive-proportional	logit
complete-matching?	TRUE	TRUE	TRUE
n-of-trials	999	999	999
single-sample?	TRUE	TRUE	TRUE
tie-breaker	uniform	uniform	uniform
log-noise-level	0	0	0.001 $S_3$
	0	0	0.05 $S_4$
	0	0	300 $S_5$
use-prob-revision?	TRUE	TRUE	TRUE
prob-revision	0.2	0.2	0.2
n-of-revisions-per-tick	500	500	500
prob-mutation	0.002	0.002	0.002
trials-with-replacement?	FALSE	FALSE	FALSE
self-matching?	FALSE	FALSE	FALSE
imitatees-with-replacement?	FALSE	FALSE	FALSE
consider-imitating-self?	FALSE	FALSE	FALSE
plot-every-?-secs	2	2	2
duration-of-recent	10	10	10
show-recent-history?	TRUE	TRUE	TRUE
show-complete-history?	TRUE	TRUE	TRUE

- $x(t)$  is a two-dimensional vector at time  $t$  which can be expressed as  $(x_m(t), x_n(t))$ , and  $x(t+1)$  is at time  $t+1$ ;
- $\times$  represents the cross product between two two-dimensional vectors.

This measurement can also be called the signed area of the the triangle  $\Delta_{[O, x(t), x(t+1)]}$  in the  $(m, n)$  two-dimensional subspace. For each transition from  $x(t)$  to  $x(t+1)$  referring to  $O$ , The angular momentum was twice that of the signed area of the triangle. We suggest using the concept of angular momentum as follows: as it contains mass as a parameter, which may be compatible with the population size  $N$  as a variable in further investigations of game dynamics.

#### 4.5. Rotation axis as the measurement

The axis of rotation is the direction of the three-dimensional angular momentum. Considering  $\sum_{i=1}^4 x_i = 1$ , we ignore  $x_4$  and let  $(x_1, x_2, x_3)$  be an independent variable. Thus, this turns out to be a three-dimensional issue. The angular momentum is the area swept by a vector per unit time. In the case of a two-dimensional

motion, the direction was perpendicular to the two-dimensional plane. To better observe the direction of the axis in the three-dimensional space, the first-, third-, and second-dimensional components of the eigenvectors are selected for calculation, and the obtained angular momentum is a three-dimensional vector. Selecting components 1, 3, and 2 for the theoretical calculation corresponds to the simulation data analysis and graphical analysis. Strategy 1 was set as the x-axis, Strategy 3 as the y-axis, and Strategy 2 as the z-axis. The formula for the theoretical calculation of angular momentum is as follows: (Zhou, 2021):

$$\bar{L} = \frac{1}{T} \int_0^T \Re(x(t)) \times \Re(v(t)) dt, \tag{18}$$

where  $x(t)$  is the strategy vector  $x$  at time  $t$ ,  $v(t)$  is the instantaneous speed of observation  $x(t)$ ,  $\Re$  is the real part,  $\times$  is the cross-multiplication, and  $\bar{L}$  is the mean angular momentum between times  $[0, T]$ . The theoretical analytical results of the axis of rotation use eigenvector components to calculate angular momentum. For each model, an arbitrarily small (e.g.,  $10^{-5}$ ) deviates from the Nash equilibrium and selects  $T \rightarrow \infty$ . It is easy to prove that this measurement is equivalent to the angular momentum measurement in Eq. (17), which can be applied to the measurements with simulation and experimental time series.

**4.6. Additional statistic test**

This section provides supplementary information on the statistical results for the main text in Section 2.4., which shows the consistency of the theory and the experiment by the measurement of the rotation direction axis vector component.

- Table 8 shows the correlation coefficients of the rotation axis for  $a = [1/4]$ ;
- Table 9 shows the correlation coefficients of the rotation axis for  $a = [4]$ .

As shown in Table 3 in the main text,  $E$  indicates the human subject experiment;  $T_i$  ( $i \in [1, 2, \dots, 5]$ ) indicates the five theoretical models;  $S_i$  ( $i \in [1, 2, \dots, 5]$ ) indicates the five-agent based simulation, respectively; for visibility, we strike out the coefficients that have relatively smaller values. This supports the results shown in the main text that, except for the models with extremely high noise parameters ( $[S_5, T_5]$ ), the theory and experiment are consistent.

**Table 8.** The correlation coefficients of the rotation axis for  $a = [1/4]$

	$T_1$	$T_2$	$T_3$	$T_4$	$T_5$	$S_1$	$S_2$	$S_3$	$S_4$	$S_5$	$E$
$T_1$	1										
$T_2$	1.000	1									
$T_3$	1.000	1.000	1								
$T_4$	0.997	0.997	0.997	1							
$T_5$	1.000	1.000	1.000	0.997	1						
$S_1$	1.000	1.000	1.000	0.997	1.000	1					
$S_2$	1.000	1.000	1.000	0.997	1.000	1.000	1				
$S_3$	0.997	0.997	0.997	1.000	0.997	0.997	0.996	1			
$S_4$	0.996	0.996	0.996	1.000	0.996	0.996	0.996	1.000	1		
$S_5$	<del>0.829</del>	<del>0.829</del>	<del>0.829</del>	<del>0.869</del>	<del>0.829</del>	<del>0.829</del>	<del>0.825</del>	<del>0.870</del>	<del>0.875</del>	1	
$E$	0.999	0.999	0.999	0.992	0.999	0.999	0.999	0.991	0.990	<del>0.798</del>	1

**Table 9.** The correlation coefficients of the rotation axis for  $a = [4]$ 

	$T_1$	$T_2$	$T_3$	$T_4$	$T_5$	$S_1$	$S_2$	$S_3$	$S_4$	$S_5$	$E$
$T_1$	1										
$T_2$	1.000	1									
$T_3$	1.000	1.000	1								
$T_4$	0.997	0.997	0.997	1							
$T_5$	0.500	0.500	0.500	0.561	1						
$S_1$	1.000	1.000	1.000	0.997	0.500	1					
$S_2$	1.000	1.000	1.000	0.998	0.507	1.000	1				
$S_3$	0.999	0.999	0.999	1.000	0.534	0.999	0.999	1			
$S_4$	0.999	0.999	0.999	0.999	0.529	0.999	1.000	1.000	1		
$S_5$	0.339	0.339	0.339	0.406	0.984	0.339	0.347	0.377	0.371	1	
$E$	0.994	0.994	0.994	0.984	0.406	0.994	0.993	0.989	0.990	0.238	1

## References

- Binmore, K., Swierzbinski, J. and Proulx, C. (2001). *Does minimax work? an experimental study*. *Economic Journal*, **111(473)**, 445–464.
- Camerer, C. (2003). *Behavioral game theory: Experiments in strategic interaction*. Princeton University Press.
- Cason, T. N., Daniel, F. and Hopkins, E. D. (2014). *Cycles and instability in a rock-paper-scissors population game: A continuous time experiment*. *Review of Economic Studies*, **81(1)**, 112–136.
- Cason, T. N., Friedman, D. and Hopkins, E. (2010). *Testing the tarp: An experimental investigation of learning in games with unstable equilibria*. *Journal of Economic Theory*, **145(6)**, 2309–2331.
- Cason, T. N., Friedman, D. and Hopkins, E. (2021). *An experimental investigation of price dispersion and cycles*. *Journal of Political Economy*, **129(3)**, 789–841.
- Friedman, D. and Sinervo, B. (2016). *Evolutionary games in natural, social, and virtual worlds*. Oxford University Press.
- Hofbauer, J., Sigmund, K., et al. (1998). *Evolutionary games and population dynamics*. Cambridge university press.
- Iyetomi, H., Aoyama, H., Fujiwara, Y., Souma, W., Vodenska, I. and Yoshikawa, H. (2020). *Relationship between macroeconomic indicators and economic cycles in us*. *Scientific reports*, **10(1)**, 1–12.
- Izquierdo, L. R., Izquierdo, S. S. and Sandholm, W. H. (2019). *An introduction to abed: Agent-based simulation of evolutionary game dynamics*. *Games and Economic Behavior*, **118**, 434–462.
- Okano, Y. (2013). *Minimax play by team*. *Games & Economic Behavior*.
- O’Neill, B. (1987). *Nonmetric test of the minimax theory of two-person zerosum games*. *Proceedings of the National Academy of Sciences*.
- Roussel, M. R. (2019). *Invariant manifolds*. In *Nonlinear Dynamics*, pp. 6-1–6-20. Morgan & Claypool Publishers.
- Sandholm, W. H. (2010). *Population Games and Evolutionary Dynamics*. MIT Press.
- Schoonbeek, L. (1987). *On the eigenvectors of macro-economic models*. *Annales d’Economie et de Statistique*, **6–7**, 335–345.
- Taylor, P. D. and Jonker, L. B. (1978). *Evolutionary stable strategies and game dynamics*. *Mathematical biosciences*, **40(1–2)**, 145–156.
- Van Huyck, J., Rankin, F. and Battalio, R. (1999). *What does it take to eliminate the use of a strategy strictly dominated by a mixture?* *Experimental economics*, **2(2)**, 129–150.
- Wang, Z. (2022). *Game dynamics structure control by design: an example from experimental economics*. arXiv preprint arXiv:2203.06088.

- Wang, Y., Chen, X. and Wang, Z. (2017). *Testability of evolutionary game dynamics based on experimental economics data*. *Physica A: Statistical Mechanics and its Applications*, **486**, 455–464.
- Wang, Z., Xu, B. and Zhou, H.-J. (2014). *Social cycling and conditional responses in the rock-paper-scissors game*. *Scientific reports*, **4(1)**, 1–7.
- Wang, Z. and Yao, Q. (2020). *Human social cycling spectrum*. arXiv preprint arXiv:2012.03315.
- Xu, B., Wang, S., and Wang, Z. (2014). *Periodic frequencies of the cycles in  $2 \times 2$  games: evidence from experimental economics*. *European Physical Journal B*, *87(2)*, 46.
- Yao, Q. (2021). *Theoretical analysis and experiment of dynamic structure of high dimensional game*. Available at: <https://cdmd.cnki.com.cn/Article/CDMD-10335-1021626407.htm>, <https://doi.org/10.27461/d.cnki.gzjdx.2021.000847> (accessed 22.08.2022);
- Zhou, S. (2021). *Theory and experiment of dynamic structure in four strategy game*. Available at: <https://cdmd.cnki.com.cn/Article/CDMD-10335-1021626406.htm> (accessed 22.08.2022); <https://doi.org/10.27461/d.cnki.gzjdx.2021.000844>.